Archives of Toxicology (2019) 93:81–93
https://doi.org/10.1007/s00204-018-2329-2

TOXICOKINETICS AND METABOLISM

A realistic human skin model to study benzo[a]pyrene cutaneous absorption in order to determine the most relevant biomarker for carcinogenic exposure

Etienne Bourgart[1] · Damien Barbeau[1,2] · Marie Marques[1] · Anne von Koschembahr[3] · David Béal[3] · Renaud Persoons[1,2] · Marie-Thérèse Leccia[4] · Thierry Douki[3] · Anne Maitre[1,2]

Received: 15 May 2018 / Accepted: 10 October 2018 / Published online: 22 October 2018

Abstract

Polycyclic aromatic hydrocarbons (PAH) are ubiquitous pollutants, among which benzo[a]pyrene (B[a]P) is the only compound classified carcinogenic to humans. Besides pulmonary uptake, skin is the major route of PAH absorption during occupational exposure. Health risk due to PAH exposure is commonly assessed among workers using biomonitoring. A realistic human ex vivo skin model was developed to explore B[a]P diffusion and metabolism to determine the most relevant biomarker following dermal exposure. Three realistic doses (0.88, 8.85 and 22.11 nmol/cm^2) were topically applied for 8, 24, and 48 h. B[a]P and its metabolites were quantified by liquid chromatography coupled with fluorimetric detection. The impact of time, applied dose, and donor age were estimated using a linear mixed-effects model. B[a]P vastly penetrated the skin within 8 h. The major metabolites were 3-hydroxybenzo[a]pyrene (3-OHB[a]P) and 7,8,9,10-tetrahydroxy-7,8,9,10-tetrahydrobenzo[a]pyrene (B[a]P-tetrol). This latter predominantly derives from the most carcinogenic metabolite of B[a]P, benzo[a]pyrene-7,8-diol-9,10-epoxide (BPDE), as well as benzo[a]pyrene-9,10-diol-7,8-epoxide (reverse-BPDE). Benzo[a]pyrene-trans-7,8-dihydrodiol (B[a]P-7,8-diol) was a minor metabolite, and benzo[a]pyrene-trans-4,5-dihydrodiol (B[a]P-4,5-diol) was never quantified. Unmetabolized B[a]P bioavailability was limited following dermal exposure since less than 3% of the applied dose could be measured in the culture medium. B[a]P was continuously absorbed and metabolized by human skin over 48 h. B[a]P-tetrol production became saturated as the applied dose increased, while no effect was measured on the other metabolic pathways. Age had a slight positive effect on B[a]P absorption and metabolism. This work supports the relevance of B[a]P-tetrol to assess occupational exposure and carcinogenic risk after cutaneous absorption of B[a]P.

Keywords Ex vivo human skin model · Polycyclic aromatic hydrocarbons · Benzo[a]pyrene · Cutaneous absorption · Metabolism · Biomonitoring

Introduction

Polycyclic aromatic hydrocarbons (PAH) are ubiquitous pollutants produced during incomplete combustion of organic matter, and distillation of coal or petroleum. They represent a large class of chemicals, consisting of more than 100

Electronic supplementary material The online version of this article (https://doi.org/10.1007/s00204-018-2329-2) contains supplementary material, which is available to authorized users.

✉ Anne Maitre
anne.maitre@univ-grenoble-alpes.fr

[1] Equipe Environnement et Prédiction de la Santé des Populations, Faculté de Médecine, Laboratoire TIMC-IMAG (UMR 5525 UGA-CNRS), Université Grenoble Alpes, 38706 La Tronche, France

[2] Service de Biochimie Biologie moléculaire Toxicologie de l'Environnement, Unité Médicale de Toxicologie Professionnelle et Environnementale, CHU Grenoble Alpes, 38000 Grenoble, France

[3] Univ. Grenoble Alpes, SyMMES/CIBEST UMR 5819 UGA-CNRS-CEA, INAC/CEA-Grenoble LAN, 38000 Grenoble, France

[4] Clinique de Dermatologie, Allergologie et Photobiologie, CHU Grenoble Alpes, 38000 Grenoble, France

compounds composed of two or more aromatic fused rings. They are emitted in the atmosphere as complex mixtures and their composition depends greatly on the emission sources (IARC 2010). In 1976, the United State Environmental Protection Agency classified 16 PAH as priority substances regarding their abundance and carcinogenicity (Andersson and Achten 2015). Amongst them, benzo[a]pyrene (B[a]P) is the only PAH to be classified "carcinogenic to humans" by the International Agency for Research on Cancer (IARC) (IARC 2010). In France, around 1.6 million workers involved in different industrial sectors are exposed to PAH, according to the 2010 SUMER study (Cavet and Leonard 2013). Besides pulmonary uptake, skin is the main occupational absorption route that can lead to high internal doses (IARC 2010). Indeed, about 51% of absorbed B[a]P resulted from skin contamination amongst coke oven workers (VanRooij et al. 1993a). Skin is an important absorption pathway due to direct contact with materials containing PAH or indirect contact with contaminated occupational uniforms or particle skin deposition (Fernando et al. 2016; Förster et al. 2008; Sobus et al. 2009). In addition to lung and bladder cancers, PAH are responsible for skin cancer developed during occupational activities, such as shale oil extraction, creosote applying, coal tar roofing and road paving, and chimney sweeping (Boffetta et al. 1997).

Dermal absorption of PAH depends greatly on their metabolism within the epidermis by cytochrome P450 mono-oxygenase (CYP450) (Ngo and Maibach 2010), including CYP1A1 and CYP1B1 (Hewitt et al. 2013). After being converted into more hydrosoluble compounds, they can easily reach the blood stream and be eliminated from the skin, whereas the diffusion of unmetabolized lipophilic PAH is limited (Jacques et al. 2010; Kao et al. 1985; Ng et al. 1992). Furthermore, PAH metabolic activation is responsible for the formation of highly mutagenic and carcinogenic metabolites in the skin (Shimada 2006). The major B[a]P bioactivation pathway begins with the formation of benzo[a]pyrene-trans-7,8-dihydrodiol (B[a]P-7,8-diol). This metabolic intermediate is involved in the o-quinone pathway, thereby producing unstable DNA adducts and reactive oxygen species (IARC 2010), and in the production of benzo[a]pyrene-7,8-diol-9,10-epoxide (BPDE), the ultimate carcinogen metabolite of B[a]P, which reacts with cellular content to form stable DNA adducts.

Occupational dermal exposure is generally assessed using "hand wiping", exposure pads, or "tape-stripping" (Fernando et al. 2016; Kammer et al. 2011; Sobus et al. 2009), but those methods evaluate skin deposition and not the amount of PAH absorbed through skin. To take into account all exposure routes and personal protective equipment, the most relevant method is the measurement of internal dose. PAH biomonitoring is routinely conducted by measuring urinary metabolites among workers using 1-hydroxypyrene which is the major metabolite of pyrene, a non-carcinogenic PAH (Jongeneelen 2001). 3-hydroxybenzo[a]pyrene (3-OHB[a]P) has been used, although this metabolite derives from a B[a]P detoxification pathway (Lutier et al. 2016). Urinary assay of 7,8,9,10-tetrahydroxy-7,8,9,10-tetrahydrobenzo[a]pyrene (B[a]P-tetrol) which reflects B[a]P bioactivation pathway has been proposed for assessing PAH carcinogenic exposure (Hecht et al. 2010; Zhong et al. 2011). However, the current issue is to confirm that these biomarkers are suitable for cutaneous exposure assessment.

Due to restrictions of animal use, ex vivo skin models were used to study cutaneous absorption and metabolism of B[a]P since in vivo and in vitro experiments demonstrate a great correlation, as long as the exposure protocols are appropriately matched (Lehman et al. 2011). However, many of those percutaneous penetration studies reflect a bias that influence B[a]P cutaneous absorption and metabolism. Since access to human skin is limited, absorption has been frequently studied using mice, rat, rabbit or guinea pig skin samples, but rodent skin was shown to more permeable to PAH than human skin (Payan et al. 2009; Storm et al. 1990 #104). Frozen skin, which is non-viable, and therefore, unable to metabolize B[a]P, was used to study PAH cutaneous absorption (Sartorelli et al. 1998). Furthermore, high exposure doses unrepresentative of human exposure are usually applied on skin, but such amounts of B[a]P decrease cutaneous absorption and saturate skin metabolism (Jacques et al. 2010; Ng et al. 1992). Finally, absorption and metabolism were mostly evaluated using radioactivity, but metabolites were rarely individually identified in those studies (Kao et al. 1985; Ng et al. 1992).

The current study had three aims: (1) the development of a representative ex vivo penetration model via freshly excised human skin for studying PAH dermal uptake pathway; (2) the investigation of cutaneous absorption and metabolism of realistic B[a]P exposure, by analysis of B[a]P and its different metabolites on the skin, in the skin, and in the culture medium; and (3) the selection of the most relevant biomarker for monitoring occupational exposure and assessing carcinogenic risk after dermal exposure.

Materials and methods

Chemicals and reagents

All aqueous solutions were prepared with water purified using the Milli-Q treatment system (Merck Millipore, Germany). Acetate buffer AVS titrinorm (pH = 4.66) solution, formic acid (HCOOH) Anala® Normapur solution (99–100%), and potassium hydroxide Prolabo® Normapur were obtained from VWR chemicals (USA). Methanol (MeOH) Chromasolv V (≥ 99.9%), B[a]P, and Bovine

Serum Albumin (BSA) came from Sigma-Aldrich (USA). Ammonium acetate and ethyl acetate RPE for analysis ACS (99.9%) were purchased from Carlo Erba Reagents (France). β-glucuronidase/arylsulfatase solution and liberase™ TH Research Grade powder were supplied by Roche Diagnostics GmbH (Germany). Gibco™ Dulbecco's Modified Eagle Medium: Nutrient Mixture F-12 (DMEM-F12), Phosphate Buffer Saline (PBS), and Gibco™ Penicillin–Streptomycin (Pen/Strep; 5.000 U/mL) were purchased from Thermo Fisher Scientific (USA). 3-OHB[a]P was obtained from LGC Standards (France). B[a]P-tetrol, benzo[a]pyrene-trans-4,5-dihydrodiol (B[a]P-4,5-diol), and B[a]P-7,8-diol were supplied by the National Cancer Institute Chemical Carcinogen Reference Standards Repository (MRIGlobal, USA).

Human skin preparation

Human skin was obtained from breast reduction surgery at Centre Hospitalier Universitaire de Grenoble, (Grenoble, France). Skin samples of 11 donors, aged from 19 to 60 years old were obtained, under informed consent and anonymous donation, in accordance with relevant guidelines and regulations. Experiments were especially conducted from article L1245-2 of the French Public Health Code on the use of surgical wastes for research purposes. Collection, storage, and use of human skin samples were declared to the French authorities and validated in the CODECOH DC-2008-444 document. After surgery, the skin was immediately transported to the laboratory within one hour at ambient temperature in 50 mL falcon tubes (Becton Dickinson Labware, USA). Skin was disinfected with PBS supplemented with 0.4% Betadine for 15 min and rinsed twice with PBS containing 10% Pen/Strep. Then, the skin was dermatomized to a thickness of 250 µm (SOBER, Humeca, Netherlands) and cut into 12-mm diameter skin discs with sterile punches (Help Medical, France). These skin biopsies included the epidermis and a minimal part of the dermis. The structural integrity on application areas was ensured, as skin damage could impact B[a]P diffusion and metabolism.

Treatment of human skin samples

Skin biopsies were placed dermal side down into polystyrene ThinCert™ inserts (14 mm inner diameter, 1 µm pore size filter, Greiner Bio-One, Austria) maintained in 12 well non-treated culture plates (Greiner Bio-One, Austria). Three doses of B[a]P (1, 10, 25 nmol, corresponding to 0.88, 8.85 and 22.11 nmol/cm^2, respectively) were applied in 5 µL of acetone on the epidermal surface. Acetone evaporation was permitted and then 500 µL of medium were added into the well, under the insert, ensuring that the epidermis was not touched. The culture medium used was DMEM-F12 supplemented with 1% Pen/Strep, and 4% BSA. Afterwards, skin biopsies were placed at 37 °C in 5% CO_2 air incubator for three different time points: 8, 24, and 48 h. For the longest exposure, the medium was removed and renewed with fresh culture medium at 24 h. Collected medium from samples was immediately stored at − 20 °C. After exposure, plates were frozen at − 80 °C to stop any metabolic activity, and then stored at − 20 °C until analysis. Experiments were performed in triplicates and were repeated on different donors' skin when possible.

B[a]P and metabolites collection from skin surface, skin, medium, and insert/well

After thawing plates at ambient temperature, skin discs were removed from inserts and placed on parafilm (Parafilm, USA, Neenah). The skin surface was softly washed twice with cotton swabs plunged in 1 mL MeOH, and then sonicated for 30 min (Bransonic® ultrasonic cleaner 5510E-MT, Branson, USA). Thirty µL MeOH were injected into high-performance liquid chromatography with fluorimetric detection (HPLC-FLD) for analysis.

After mincing skin samples and adding 1 mL acetate buffer (pH = 7.4), skin was digested with 1 U/mL Liberase™ TH enzyme at 37 °C for 2 h. One mL of acetate buffer (pH = 4.66) was added, and the skin was next ground with an ultra turrax (IKA werke®, Germany), then incubated with 30 µL β-glucuronidase/arylsulfatase at 37 °C for 30 min. The next step was skin saponification in 1M of potassium hydroxide at 60 °C for 1 h. After cooling at ambient temperature, B[a]P and its metabolites were extracted by liquid–liquid extraction. Two millilitres of ethyl acetate saturated with water were added. Mixture was placed on rotary agitator for 30 min, and then centrifuged at 4000 rpm for 10 min at 4 °C. The upper phase corresponding to the organic phase was recovered. The liquid–liquid extraction was repeated twice, and the organic phases were pooled before a 1:4 dilution in MeOH. Thirty µL were injected into HPLC–FLD. The recovery of B[a]P and metabolites extracted from the skin was assessed using untreated skin samples spiked with B[a]P and metabolites reference standards before applying the whole extraction protocol.

The medium was removed from the well and pooled with the related previous medium stored at − 20 °C in the case of a 48 h exposure. Hydrolysis step of conjugated metabolites was performed by adding 50 µL acetate buffer (pH 4.66) and 10 µL β-glucuronidase arylsulfatase to 100 µL of the medium by incubation at 37 °C for 2 h. This step was stopped by addition of 150 µL MeOH. After sample centrifugation at 4000 rpm for 10 min at 4 °C, 30 µL of the supernatant was injected into HPLC. Alongside this procedure, inserts and wells were washed and sonicated twice for 2 min with 1 mL MeOH. Thirty µL was injected into HPLC-FLD for analysis.

HPLC analysis of B[a]P and its metabolites

The analysis of B[a]P and its metabolites was performed using a HPLC Waters® (USA) Model 2695 separation module equipped with a quaternary pump, a thermostated compartment for the chromatographic column, an autosampler, an automatic injector, and an integrated degasser. Fluorescence detection was performed with a Waters® 2475 multi-wavelength detector. A Waters® PAH-C18 column (3.0 × 250 mm, 3 µm) was used for analytes separation. The column temperature was maintained at 30 °C and samples temperature at 12 °C. Mobile phases, used at a flow-rate of 0.5 mL/minute, consisted of formic acid (13,2 µM), and MeOH. The gradient of mobile phases is described in Table 1. Excitation and emission wavelengths were fixed at: 345 and 389 nm for B[a]P-Tetrol, 265 and 365 nm for B[a]P-4,5-diol, 349 and 398 nm for B[a]P-7,8-diol, 365 and 430 nm for 3-OHB[a]P, and 296 and 405 nm for B[a]P, respectively.

Data analysis

Concentrations of B[a]P and metabolites below the quantification limit (QL) were replaced by the half of the QL value. Their levels were expressed in the percentage of the applied dose. The results were presented in 3 parts: unmetabolized B[a]P distribution in human skin model, B[a]P-tetrol/B[a]P ratios in skin and culture medium, and metabolites production by human skin. In each part, results were graphically presented before describing modelling results. Figures were created using Microsoft Excel or R 3.3.2 software.

Due to repeated measures, either at the same time (replicates) or at different times (from 8 to 48 h) and the inclusion of several donors, linear mixed effects models were used. Data analysis was performed using R 3.3.2 software (R foundation for Statistical Computing). The normality of the distributions was ensured or approached using Shapiro–Wilk test following Box-Cox transformation. Metabolites data obtained after 8 h exposures were excluded from the model as a great majority of concentrations were below the QL: B[a]P-tetrol was below the QL for all the skin samples while B[a]P-tetrol, B[a]P-7,8-diol, and 3OHB[a]P were below the QL in 21, 20, and 24 out of 24 medium samples, respectively. The relations between B[a]P dose, time, and age of donors with total unmetabolized B[a]P (B[a]P on skin surface, in skin, and adsorbed on the insert/well), unmetabolized B[a]P and metabolites in the medium, B[a]P-tetrol/B[a]P ratios in the skin and in the medium were studied using the "lme" function from "nlme" package (Pinheiro and Bates 2000). B[a]P dose, time, and age of donors were included as fixed effects, while random effects were defined by replicates nested in the same subject's samples. Data from 24 to 48 h exposures were compared to those of 8 and 24 h exposures, respectively, while data from 10 nmol-exposure and 25 nmol-exposure were both compared to those of 1 nmol-exposure. For all tests, a p value below 0.05 was considered significant.

Table 1 Composition of mobile phases and gradient curves during the whole run

Time (min)	Mobile phases		Gradient curves
	Formic acid (%)	MeOH (%)	
0.0	90.0	10.0	Convex ($n = 1/3$)
1.0	90.0	10.0	Convex ($n = 1/3$)
–	↓	↓	Convex ($n = 1/3$)
21.0	0.0	100.0	Convex ($n = 1/3$)
24.0	0.0	100.0	Linear ($n = 1$)
–	↓	↓	Linear ($n = 1$)
25.0	90.0	10.0	Linear ($n = 1$)
35.0	90.0	10.0	Linear ($n = 1$)

↓: gradient in progress. % of MeOH variation was calculated by the Waters® software according to the following equation:

$$\%B = \%B_{\text{initial}} + \left(\%B_{\text{final}} - \%B_{\text{initial}}\right) \times \left(\frac{\%T}{100}\right)^{n}$$

%T is percentage of time passed in the gradient segment, n is described for each gradient curve

Results

Analysis and skin extraction efficiency of B[a]P and its metabolites

B[a]P and its four metabolites were well separated by HPLC coupled with fluorescence detection (Fig. 1). The QL for B[a]P-tetrol, B[a]P-4,5-diol, B[a]P-7,8-diol, 3-OHB[a]P, and B[a]P were 0.07, 0.14, 0.08, 0.13 and 0.31 ng/mL, respectively.

The recoveries for B[a]P, B[a]P-tetrol, and B[a]P-4,5-diol from skin samples spiked with standards were 99.2 ± 0.5%, 105.0 ± 1.3% and 106.5 ± 2.8% ($n = 9$), respectively. However, B[a]P-4,5-diol was always below the QL in the skin or medium samples. On the contrary, 3-OHB[a]P recovery from skin was very low (extraction mean = 5.9 ± 1.5%; $n = 9$), and B[a]P-7,8-diol recovery was variable (extraction mean = 60.6 ± 16.0%; $n = 9$). Besides B[a]P, B[a]P-tetrol was the only metabolite that could be quantified in the skin, while B[a]P-tetrol, B[a]P-7,8-diol, and 3-OHB[a]P could be analysed in the medium.

Unmetabolized B[a]P distribution in the 4 compartments of the skin model

The distribution of unmetabolized B[a]P quantified in the four compartments of skin model after B[a]P exposure at

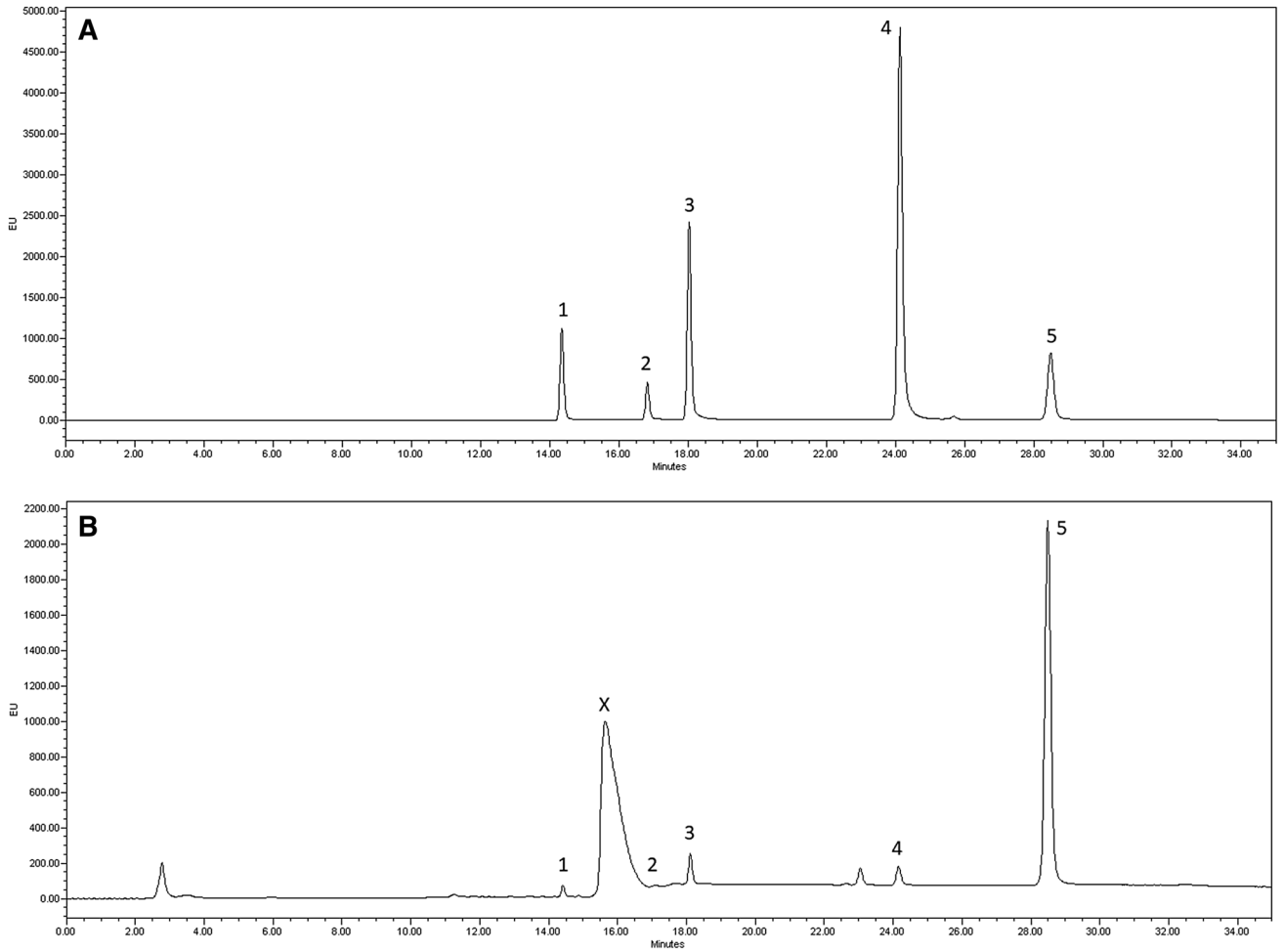

Fig. 1 Chromatographic separation of (1) B[a]P-tetrol, (2) B[a]P-4,5-diol, (3) B[a]P-7,8-diol, (4) 3-OHB[a]P and (5) B[a]P after injection of (A) standards mixture, (B) culture medium sample of human skin explants exposed to B[a]P (25 nmol, 24 h). *X* unknown impurity

different doses (1, 10, 25 nmol), and at different exposure times (8, 24, 48 h) is presented on Fig. 2. The percentage of total unmetabolized B[a]P out of the applied dose globally decreased with the exposure time, whatever the dose. While the percentage was around 95% after 8 h exposure for all the doses, it ranged from 54 to 94% at 24 h and from 22 to 48% at 48 h, according to the dose.

The percentage of B[a]P remaining on the skin surface reduced with increasing exposure time. For 1 nmol, B[a]P decreased from 25% after 8 h to 10–15% after 24 and 48 h. For 10 and 25 nmol, the decline was more important as the percentage of B[a]P decreased from 45% after 8 h to 3% after 48 h of exposure. The percentage of B[a]P remaining on the skin surface rose with increasing applied dose for the two first exposure times. After 8 h, B[a]P found on the skin surface was about 28% for 1 nmol, while it was 45% for 10 and 25 nmol. After 24 h, B[a]P on the skin surface was 2–3 times higher for 25 nmol than for 1 and 10 nmol. The percentage of B[a]P measured in the skin varied according to applied dose and exposure time. At 8 h of exposure, 64% of the applied dose was located in the skin for 1 nmol, while it was around 43% for 10 and 25 nmol. The decrease of unmetabolized B[a]P with rising exposure time seemed faster for 1 nmol than for the two other doses. Indeed, after 24 and 48 h, 32% and 9% of applied dose were in the skin for 1 nmol, respectively. For 10 and 25 nmol, 45% and 55% remained in the skin after 24 h, respectively, and then decreased to 12% and 35% after 48 h. B[a]P in the medium and on the insert/well remained below 3% and 12%, respectively, whatever the time and dose.

The impact of applied dose and exposure time on unmetabolized B[a]P quantified in the different compartments of skin model was analysed using a linear mixed-effect model (Table 2). Results confirmed that total unmetabolized B[a]P and B[a]P remaining on the skin surface decreased as exposure time increased. For total unmetabolized B[a]P, a very high negative coefficient (− 16) was calculated for the 8–24 h period, and it was multiplied by two during the

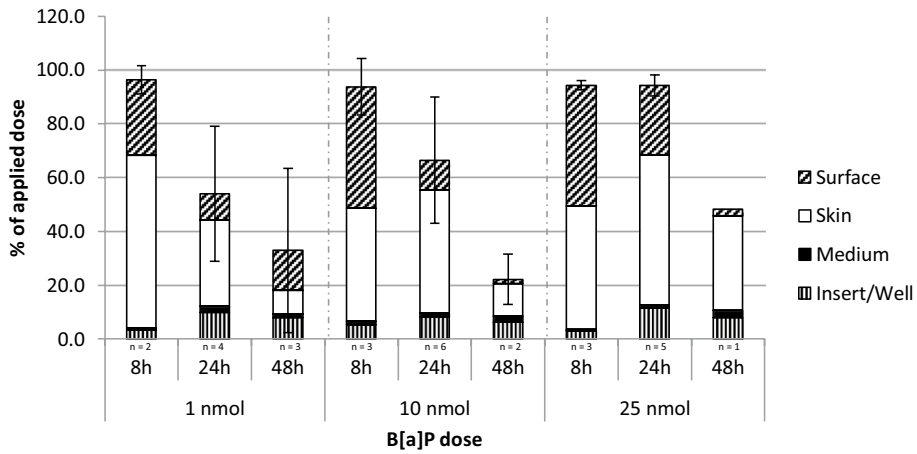

Fig. 2 Unmetabolized B[a]P distribution in human skin model in function of exposure time and topically applied dose. Data are expressed in the percentage of applied dose (n = number of donors, mean of donors ± standard deviation of donors' mean total recovery)

24–48 h period. Coefficients for skin surface were lower (− 2), but comparable for the 2 time periods. While time had a great negative effect (− 9) on unmetabolized B[a]P found in the skin during the second period, it had no significant effect during the first period. On the contrary, time had a low, positive impact (+ 0.5) on B[a]P found in the medium for the two time periods. While it had a low positive impact on B[a]P found on the insert/well during the first period, it had a low negative effect for the second.

The increase of B[a]P applied dose had an important positive effect on total unmetabolized B[a]P. The coefficient which was around + 10 when the dose increased from 1 to 10 nmol, was multiplied by two when the dose rose from 10 to 25 nmol. A moderate positive effect (+ 1.5) of applied dose was observed on B[a]P remaining on skin surface for the 2 dose increases. For B[a]P in the skin, only the highest dose had a great significant positive effect (+ 3.5), although the intermediate dose was close to being statistically significant. Conversely, applied dose did not influence the percentage of B[a]P found in the medium or on the insert/well.

Age had a roughly positive effect on the B[a]P found in the medium. Inter-individual variability was higher than residual variability, except in the skin.

B[a]P-tetrol/B[a]P ratios in skin and culture medium

The ratios of B[a]P-tetrol level out of B[a]P level found in skin and in medium were calculated after B[a]P exposure at different doses (1, 10, 25 nmol) and different exposure times (8, 24, 48 h) (Fig. 3). After an 8 h exposure, the ratios were close to zero in the skin and in the medium, whatever the dose applied. These ratios increased over time in the skin and in the medium, but increases in the medium were higher than those in the skin. However, these increases were lower when the applied dose was extended, whether in the skin or in the medium. While the ratios reached 0.23 in the skin and 1.05 in the medium for 1 nmol after 48 h exposure, they were 2–3 times lower for 10 nmol, and 5–6 times lower for 25 nmol, respectively.

These results were confirmed using a linear mixed effects model (Table 3). Time had a positive effect on the B[a]P-tetrol/B[a]P ratios, while increasing applied dose had a negative effect, whether in the skin or in the culture medium. The coefficient which was equal to − 0.8 when the dose increased from 1 to 10 nmol, was multiplied by two when the dose raised from 10 to 25 nmol. These coefficients were in the same order of magnitude in the skin and in the medium. Age had no effect on B[a]P-tetrol/B[a]P ratio. While inter-individual variability was twice lower than residual variability in the skin, it was comparable in the medium.

B[a]P metabolites in the culture medium

B[a]P-tetrol, B[a]P-7,8-diol and 3-OHB[a]P were quantified in the medium following B[a]P exposure at different doses (1, 10, 25 nmol) and different exposure times (8, 24, 48 h) (Fig. 4). B[a]P-tetrol and 3-OHB[a]P were the main metabolites released at comparable levels in the medium, while B[a]P-7,8-diol levels were around seven times lower. The percentage of B[a]P-tetrol and 3-OHB[a]P out of the total B[a]P applied dose increased in the medium with exposure time. B[a]P-tetrol production was lower when the B[a]P applied dose increased after 24 and 48 h exposure times, whereas this difference was unclear for 3-OHB[a]P after 48 h.

Data analysis with a linear mixed effects model confirmed that the levels of B[a]P-tetrol and 3-OHB[a]P increased during the 24–48 h period (+ 1.4), whereas this factor had a lower negative effect on B[a]P-7,8-diol production (− 0.6) (Table 4). Increasing the B[a]P applied dose had no effect on 3-OHB[a]P and B[a]P-7,8-diol production, whereas it had a negative effect on B[a]P-tetrol production. The coefficient, which was equal to − 0.5 when the dose increased from 1 to 10 nmol, was doubled when the dose raised from 10 to

Table 2 Results from linear mixed effects models for total unmetabolized B[a]P (skin surface + skin + medium + insert/well), B[a]P remaining on skin surface, B[a]P in skin, B[a]P in medium and B[a]P adsorbed on insert/well

	Total		Skin surface		Skin		Medium		Insert/well	
	Estimate (SE)	*p* value	Estimate (SE)	*p* value	Estimate (SE)	*p* value	Estimate (SE)	*p* value	Estimate (SE)	*p* value
Intercept	77.394 (21.277)	**0.001**	7.236 (2.338)	**0.003**	11.466 (3.861)	**0.005**	− 1.753 (0.908)	0.059	1.694 (0.864)	0.055
Age	− 0.570 (0.489)	0.274	− 0.103 (0.054)	0.091	− 0.035 (0.088)	0.698	0.049 (0.021)	**0.044**	0.003 (0.020)	0.871
Dose										
1	Ref		Ref		Ref		Ref		Ref	
10	10.990 (4.457)	**0.017**	1.152 (0.249)	**0.000**	1.826 (0.942)	0.058	− 0.097 (0.172)	0.577	− 0.109 (0.176)	0.539
25	21.073 (5.914)	**0.001**	1.721 (0.338)	**0.000**	3.600 (1.249)	**0.006**	0.189 (0.229)	0.412	0.059 (0.233)	0.800
Time										
24–8	− 16.088 (4.868)	**0.002**	− 2.207 (0.274)	**0.000**	0.731 (1.025)	0.479	0.390 (0.189)	**0.044**	0.789 (0.192)	**0.000**
48–24	− 39.726 (4.676)	**0.000**	− 2.389 (0.267)	**0.000**	− 8.670 (0.984)	**0.000**	0.500 (0.181)	**0.008**	− 0.549 (0.184)	**0.004**
Random effects										
σ_b^2	339.566		4.515		10.632		0.633		0.547	
Residual	225.225		0.672		10.263		0.334		0.349	

Significant *p* values are in bold

SE standard error, σ_b^2 inter-individual variability

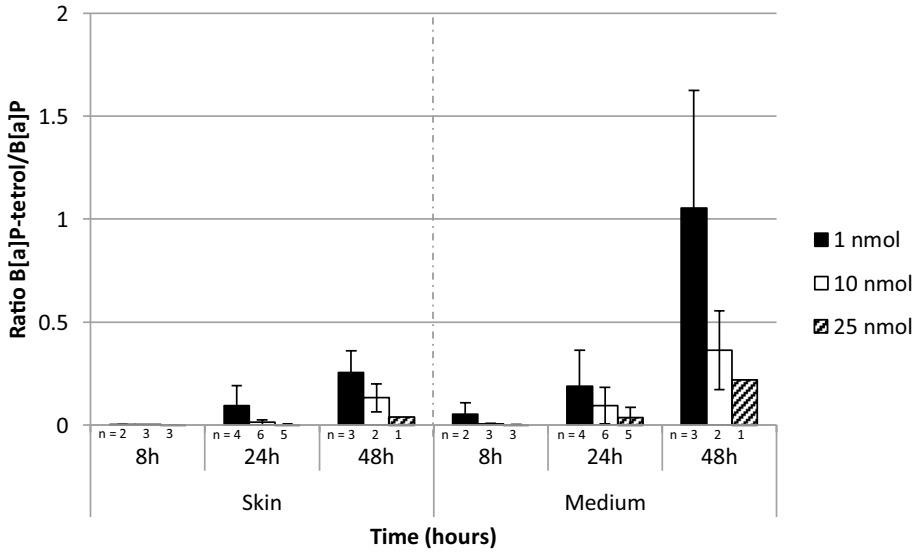

Fig. 3 Ratios B[a]P-tetrol/B[a]P in skin and medium in function of exposure time (n = number of donors, mean of donors ± standard deviation)

Table 3 Results from linear mixed effects model for the ratios B[a]P-tetrol/B[a]P calculated in the skin and in the medium

	Skin		Medium	
	Estimate (SE)	p value	Estimate (SE)	p value
Intercept	− 3.094 (0.536)	**0.000**	− 0.918 (0.756)	0.234
Age	0.026 (0.012)	0.067	− 0.002 (0.018)	0.898
Dose				
1	Ref		Ref	
10	− 0.833 (0.172)	**0.000**	− 0.739 (0.210)	**0.001**
25	− 1.454 (0.220)	**0.000**	− 1.392 (0.265)	**0.000**
Time				
48–24	1.226 (0.147)	**0.000**	0.977 (0.177)	**0.000**
Random effects				
σ_b^2	0.159		0.353	
Residual	0.234		0.328	

Significant p values are in bold

SE standard error, σ_b^2 inter-individual variability

25 nmol. Age had a slight positive effect on the production of B[a]P-tetrol and 3-OHB[a]P, but had no influence on B[a]P-7,8-diol formation. Inter-individual variability was lower than residual variability for B[a]P-tetrol and 3-OHB[a]P, while it was higher for B[a]P-7,8-diol.

Discussion

Dermal uptake is a major concern in pharmaceutical and toxicological sciences. Increasing restrictions in animal testing has led to the development of diversified in vitro skin models, from artificial membrane and reconstructed human skin models to ex vivo skin models (Flaten et al. 2015). In the present study, using ex vivo samples from freshly excised human skin serves as the best representative model to reproduce realistic cutaneous exposure in humans. Moreover, it suppresses the uncertainty between species (Kao et al. 1985;

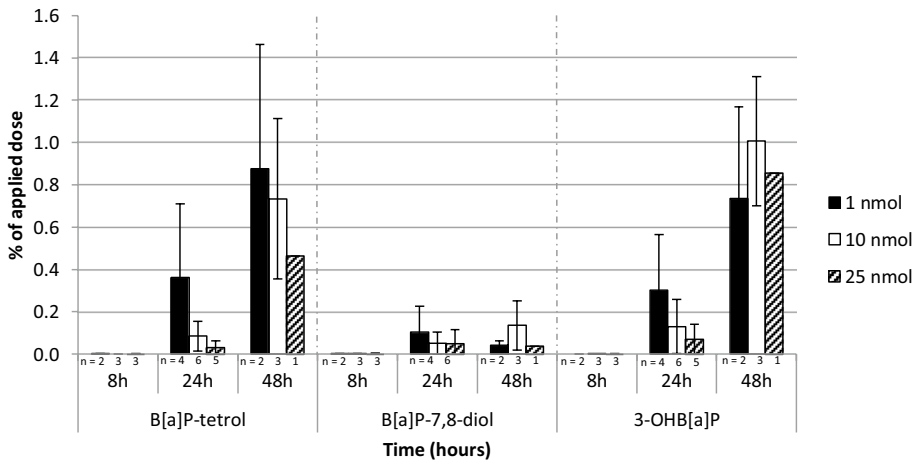

Fig. 4 Appearance of B[a]P-tetrol, B[a]P-7,8diol and 3-OHB[a]P in medium as a function of time. Data are expressed in % of applied dose (n = number of donors, mean of donors ± standard deviation)

Table 4 Results from linear mixed effects models for B[a]P-tetrol, B[a]P-7,8-diol and 3-OHB[a]P in medium

	B[a]P-tetrol		B[a]P-7,8-diol		3-OHB[a]P	
	Estimate (SE)	*p* value	Estimate (SE)	*p* value	Estimate (SE)	*p* value
Intercept	− 2.808 (0.546)	**0.000**	3.285 (1.095)	**0.005**	− 2.713 (0.339)	**0.000**
Age	0.044 (0.013)	**0.008**	− 0.021 (0.026)	0.437	0.042 (0.007)	**0.000**
Dose						
1	Ref		Ref		Ref	
10	− 0.533 (0.176)	**0.005**	− 0.142 (0.195)	0.473	− 0.059 (0.160)	0.714
25	− 1.006 (0.224)	**0.000**	0.341 (0.244)	0.171	− 0.325 (0.208)	0.128
Time						
48–24	1.425 (0.150)	**0.000**	− 0.634 (0.163)	**0.000**	1.423 (0.141)	**0.000**
Random effects						
σ_b^2	0.165		0.861		0.026	
Residual	0.243		0.259		0.254	

Significant *p* values are in bold

SE standard error, σ_b^2 inter-individual variability

Payan et al. 2009). The use of human skin is cumbersome, since the experimental plan has to be adapted to the operating program of surgeons, as well as to the size and quality of skin biopsies obtained following surgery. Acetone was chosen as the deposition vehicle, as in number of studies (Brinkmann et al. 2013; Jacques et al. 2010; Moody et al. 2009). A restricted volume (5 µL) was applied on the skin to limit its impact on cutaneous absorption and metabolism (Ibrahim and Li 2009; Kontir et al. 1986). Culture plates with inserts (static membranes) were used because this model of organ culture system maintains the skin at an air–liquid interface and nutrients diffuse across the insert to feed the dermis/epidermis. Additionally, numerous experimental conditions can be conducted simultaneously and low amounts of xenobiotics can be applied (Jacques et al. 2010). Other systems were used in the literature as Franz cells (static cells) or flow-through cells (dynamic cells) (Kao et al. 1985), but no difference was showed between them (Bronaugh and Stewart 1985; van de Sandt et al. 2004). The proportion of B[a]P recovered from the insert/well was comparable to those previously measured (Jacques et al. 2010).

Breast skin was recovered immediately after plastic surgery, whereas other studies were usually conducted on abdominal skin (Brinkmann et al. 2013; Hopf et al. 2018; Payan et al. 2009; Storm et al. 1990), but differences in PAH permeation between anatomical skin sites were low in humans in vivo (VanRooij et al. 1993b). Moreover, breast skin was reproducibly dermatomized to 250 µm with a SOBER mechanical dermatome while other anatomical pieces, such as abdominal skin, require the use of an electrodermatome, due to higher thickness and resistance (Brinkmann et al. 2013; Hopf et al. 2018; Payan et al. 2009). A thickness of 250 µm was chosen because most of the absorbed chemicals enter the bloodstream through the skin capillaries located in the dermis at a depth of 200 µm (Bronaugh and Stewart 1986). This is in agreement with the literature, as most authors use a skin thickness ranging from 200 µm to 500 µm (Jacques et al. 2010; Ng et al. 1992; Payan et al. 2009; Storm et al. 1990). Unmetabolized B[a]P in the medium, as substitute of B[a]P uptake, was limited and remained below 3% of the applied dose. This result demonstrated the great importance of metabolism in B[a]P cutaneous absorption. Similar results were previously obtained using either human or pig skin (Jacques et al. 2010; Moody et al. 2009). A study recently confirmed that unmetabolized B[a]P diffusion through human skin was limited, while lighter and thus more hydrosoluble PAH were shown to cross human skin more easily (Hopf et al. 2018). Since B[a]P is a lipophilic compound, special attention was made to help its partitioning in the medium, while avoiding components likely to artificially influence skin metabolism, such as fetal bovine serum. Indeed, absence of substances helping the diffusion of lipophilic compounds was responsible for the quantification of B[a]P traces only (Brinkmann et al. 2013). Thus, BSA was added to the medium, as previously published (Jacques et al. 2010; Moody et al. 1995; Payan et al. 2009). Unmetabolized B[a]P uptake increased over time, but the dose had no significant effect on the proportion in the medium, demonstrating the proportionality to applied dose up to 25 nmol in accordance with a passive diffusion mechanism. Due to a great first-pass metabolism, unmetabolized B[a]P is poorly bioavailable following dermal exposure, which indicates that B[a]P carcinogenicity is mostly located on the skin contamination site.

Skin samples were recovered from the hospital and treated within two hours to ensure viability. This operating mode was previously shown to conserve skin integrity using transepidermal water loss measurements (Hopf et al. 2018). In this study, human skin metabolized B[a]P to a great extent, especially after 24 h. This time point corresponds

with the maximum activity of CYP450 enzymes in human skin following a treatment with coal tar (Bickers and Kappas 1978). CYP450 production is dependent of the activation of aryl hydrocarbon receptor (AhR) via PAH binding to the AhR complex (Moorthy et al. 2015), resulting in a latency in their production (Genies et al. 2013). The core of the present study was the specific analysis of four B[a]P metabolites selected as potential biomarkers, according to the current literature. B[a]P-tetrol and B[a]P-7,8-diol were selected for the evaluation of B[a]P carcinogenic bioactivation. B[a]P-7,8-diol constitutes the proximate carcinogenic metabolite of B[a]P, while B[a]P-tetrol is the hydrolysis product of both the ultimate carcinogen, BPDE, and the non-carcinogenic reverse-BPDE. B[a]P-tetrol quantified in the present study corresponded to the sum of the two enantiomers deriving from BPDE (B[a]P-(7R,8S,9R,10S)-tetrol) and reverse-BPDE (B[a]P-(7S,8R,9S,10R)-tetrol). Nevertheless, the B[a]P-(7R,8S,9R,10S)-tetrol enantiomer represented 78% of B[a]P-tetrol measured in the urine of occupationally exposed creosote workers (Hecht et al. 2010). Therefore, racemic B[a]P-tetrol analyzed in this study seems to be a relevant PAH exposure biomarker linked to the B[a]P proportion involved into carcinogenic BPDE pathway (Barbeau et al. 2017). 3-OHB[a]P is used as biomarker of exposure among occupationally exposed workers and represent a detoxification pathway (Barbeau et al. 2011; IARC 2010). Along with B[a]P-4,5-diol, those two metabolites are used as biomarkers for in vivo studies (Moreau and Bouchard 2014). B[a]P-9,10-diol was excluded as potential biomarker, contrary to other studies (Brinkmann et al. 2013), as this metabolic intermediate belongs to the reverse-BPDE pathway and was not detected in rat urine following exposure to B[a]P (Bouchard and Viau 1996). Three of these metabolites (B[a]P-7,8-diol, B[a]P-tetrol, and 3-OHB[a]P) were quantified in the culture medium while B[a]P-4,5-diol was constantly below the QL. Although B[a]P-4,5-diol was the second major metabolite in rats, this is consistent with *in vitro* studies showing limited formation in humans (Plakunov et al. 1987; Schwarz et al. 2001). B[a]P-tetrol and 3-OHB[a]P were the two major metabolites, steadily produced by human skin at comparable levels, whereas B[a]P-7,8-diol production was minor. Levels of B[a]P-tetrol and 3-OHB[a]P increased over time, while time had a low negative effect on the production of B[a]P-7,8-diol. 3-OHB[a]P was the major metabolite in vivo in rats after cutaneous exposure to B[a]P, while B[a]P-7,8-diol was minor and B[a]P-tetrol was barely detectable (Moreau and Bouchard 2014). B[a]P-7,8-diol is an intermediate metabolite involved in several metabolic pathways (Penning 2014); further metabolism could thus explain its low levels. Brinkmann *et al*. obtained a different metabolic profile after application of 50 nmol/cm^2 of B[a]P on abdominal human skin explants. B[a]P-7,8-diol was among the major metabolites whereas 3-OHB[a]P and B[a]P-tetrol were the minor metabolites. This discrepancy in the metabolic profile probably comes from differences in experimental procedures. Brinkmann et al. used the EFT-400-ASY medium designed by MatTek for the production and maintenance of EpiDerm-FT™, a reconstituted human skin model (Brinkmann et al. 2013). Among other components (epidermal growth factor and other proprietary stimulators of epidermal differentiation), the medium composition includes hormones (insulin and hydrocortisone) and lipid precursors added to induce cellular growth and differentiation, but which may also be involved in the regulation of CYP450 expression (Zanger and Schwab 2013). A previous *in vitro* study underlined the dramatic impact of various hormones (triiodothyronine and growth hormone) on the expression of CYP3A4 by primary cultured hepatocytes (Liddle et al. 1998). In addition, the absence of BSA in the EFT-400-ASY medium greatly impacts the metabolic profile measured from the medium. Thus, in preliminary experiments in our study, 3-OHB[a]P and B[a]P-tetrol levels were respectively divided by 8.5 and 1.5 when BSA was excluded from medium composition (Fig. S2). This discrepancy may also result from the use of explants coming from different anatomic regions. Nevertheless, the few data available in the literature demonstrates a relatively even skin metabolism according to anatomic site and equal constitutive expression of xenobiotic metabolizing enzymes between breast and abdominal skin (Cheung et al. 1999; VanRooij et al. 1993b). The increase of metabolite levels after 48 h demonstrates that skin is viable at the end of exposure, as previously described with pig skin (Jacques et al. 2010).

With the goal of representing occupational exposures while being able to measure metabolites, two low B[a]P doses (0.88 and 8.85 nmol/cm^2) and one high dose (22.12 nmol/cm^2) for comparison with the literature, were deposited on skin explants. Indeed, applied doses usually ranged from 6 to 293 nmol/cm^2, with a great majority higher than 30 nmol/cm^2 (Brinkmann et al. 2013; Jacques et al. 2010; Kao et al. 1985; Ng et al. 1992; Payan et al. 2009). In our study, the deposited amounts were close to dermal exposures measured in industrial settings using coal tar raw material. Dermal contamination remained below 5 fmol/cm^2 for asphalt workers (Fustinoni et al. 2010), whereas it reached 1 nmol/cm^2 for workers exposed to coal tar in aluminium production or roofing (Mcclean et al. 2006; VanRooij et al. 1992). Results demonstrate a great permeability of human skin up to 25 nmol. More than half of the applied dose penetrated the skin within 8 h, which corresponds to the duration of a full working day. The remaining B[a]P steadily penetrated the skin, since lipophilic compounds like B[a]P accumulate in the stratum corneum by passive diffusion, resulting in a skin reservoir (Bronaugh and Maibach 2005; Chu et al. 1996). However, B[a]P penetration and metabolism were slower at higher doses resulting in unmetabolized

B[a]P accumulation both in and on the skin, which was also demonstrated on pig skin over 50 nmol/cm^2 and hairless guinea pig skin over 32 nmol/cm^2 (Jacques et al. 2010; Ng et al. 1992). The decrease in penetration at high doses may indicate a saturation of the skin reservoir. As a result, Moody et al. measured more than 40% of B[a]P remaining on the skin surface after an application of 39 nmol/cm^2 for 24 h (Moody et al. 1995). B[a]P-tetrol metabolic pathway was saturated above 0.88 nmol/cm^2, whereas no significant effect was observed on 3-OHB[a]P formation. Indeed, sulfate and glucuronide conjugated 3-OHB[a]P and 9-OHB[a]P were the major metabolites after application of high doses of B[a]P on pig skin, whereas B[a]P-tetrol represented only a limited amount of metabolites. Comparatively to B[a]P-tetrol, the saturation of OH-B[a]P glucuronide and sulfate conjugates production observed with pig skin started over 200 nmol/cm^2 (Jacques et al. 2010). This limitation in B[a]P-tetrol production may be due to a saturation of epoxide hydrolase (EH). Indeed, B[a]P conversion to B[a]P-tetrol requires three successive biochemical reactions involving xenobiotic metabolizing enzymes like CYP1A1/1B1 and EH to form BPDE, and a spontaneous hydrolysis step from BPDE to B[a]P-tetrol. In contrast, 3-OHB[a]P metabolism counts only one step involving CYP450 to form arene oxide (Shimada 2006; Zhong et al. 2011), and a spontaneous non enzymatic rearrangement from intermediate arene oxide to phenol. The saturation in B[a]P-tetrol production indicates a limitation of BPDE metabolic pathway as the applied dose increases. In vitro, BPDE adducts were quantitatively the main mechanism of B[a]P carcinogenicity, whereas *o*-quinone and radical cation pathways were minor contributors even when the dose increased (Genies et al. 2013). In addition, DNA adducts produced during the radical cation pathway is a minor activation mechanism of PAHs in vivo (Xue and Warshawsky 2005). Altogether, this may indicate that B[a]P carcinogenicity might not increase even when skin contamination increases (in concentration or number of exposure times). These results demonstrate that the applied dose has a great influence on B[a]P metabolism and needs to be carefully discussed before using data of in vitro or in vivo model for human risk assessment. The importance of metabolic considerations in the use of in vitro skin model for risk assessment was previously underlined (Hewitt et al. 2013).

Data analysis was ensured using a linear mixed-effect model to take into account the use of the 11 different skin donors. The accuracy of the linear mixed effect model was confirmed by homoscedasticity distributions of standardized residues over fitted values (Fig. S1). Besides underlining the significant trends, the linear mixed effect model quantified the inter-individual and the residual variabilities in B[a]P skin absorption and metabolism. A high inter-individual variability was observed for unmetabolized B[a]P penetration as various skin donors were exposed to different applied doses during various durations. Inter-individual variability in B[a]P uptake was rather limited, contrary to previous studies (Hopf et al. 2018; Payan et al. 2009). Donors' ages were declared as a fixed effect, although it only had a limited impact on permeation and metabolism. In the literature, high inter-individual variabilities are also described toward skin absorption of numerous other drugs (Farahmand and Maibach 2009). Several factors contribute to inter-individual variability such as ethnicity, gender, genotype, general health, local blood flow, and formation and duration of skin depot (Aklillu et al. 2005; Farahmand and Maibach 2009; Payan et al. 2009; Shimada 2006). Residual variability was sometimes higher than inter-individual variability, since intra-individual variability, as well as analytical or experimental imprecisions were not defined in the model. This increase in model error remained limited since variances were low in such cases.

Conclusion

Ex vivo human skin models are relevant to study absorption and metabolism of xenobiotics after cutaneous exposure, but our results highlight the great influence of applied dose and experimental conditions on skin absorption assays. Due to the large amount of B[a]P cutaneous absorption, wearing protective equipment during occupational activities is essential, as well as skin decontamination following work completion. Unmetabolized B[a]P and B[a]P-7,8-diol are not good biomarkers. Indeed, samples can become contaminated by B[a]P when collecting at the workplace. Moreover, B[a]P uptake was limited, while B[a]P-7,8-diol was a minor metabolite. Conversely, both 3-OHB[a]P and B[a]P-tetrol are the two major metabolites found in the culture medium and these biomarkers can be quantified in the urine of workers exposed to PAH. For assessing carcinogenic risk, racemic B[a]P-tetrol is more relevant than 3-OHB[a]P because it is representative of the main B[a]P bio-activation pathway. Furthermore, B[a]P-tetrol metabolic pathway was rapidly saturated, whereas no significant effect was observed on 3-OHB[a]P formation. Thus, the quantification of this last metabolite could overestimate the carcinogenic risk when skin contamination increase, due to increased concentrations or occurrences. Due to metabolism interactions of different PAH and other pollutants present in complex mixtures emitted by occupational and environmental sources, further studies are required to evaluate cutaneous absorption and metabolism of B[a]P using commercial products used in different types of companies.

Acknowledgements This work was funded by the French National Institute of Health and Medical Research (INSERM) (Grant Number ENV201412) and Plan Cancer. The authors wish to thank the team

"Service de Chirurgie Plastique et Maxillo-faciale CHU Grenoble Alpes" for their help in skin sample collection.

Compliance with ethical standards

Conflict of interest The authors declare that they have no conflict of interest.

Ethical approval Experiments were conducted in accordance with the article L1245-2 of the French Public Health Code on the use of surgical wastes for research purposes. Collection, storage, and use of human skin samples were made anonymously, declared to the French authorities, and validated in the CODECOH DC-2008-444 document.

Informed consent Informed consent was obtained from all skin donors.

References

Aklillu E, Øvrebø S, Botnen IV, Otter C, Ingelman-Sundberg M (2005) Characterization of common CYP1B1 variants with different capacity for Benzo[a]pyrene-7,8-dihydrodiol epoxide formation from Benzo[a]pyrene. Cancer Res 65(12):5105–5111 https://doi.org/10.1158/0008-5472.can-05-0113

Andersson JT, Achten C (2015) Time to Say goodbye to the 16 EPA PAHs? Toward an up-to-date use of PACs for environmental purposes. Polycyclic Aromat Compd 35(2–4):330–354. https://doi.org/10.1080/10406638.2014.991042

Barbeau D, Lutier S, Choisnard L, Marques M, Persoons R, Maitre A (2017) Urinary trans-anti-7,8,9,10-tetrahydroxy-7,8,9,10-tetrahydrobenzo(a)pyrene as the most relevant biomarker for assessing carcinogenic polycyclic aromatic hydrocarbons exposure. Environ Int 112:147–155. https://doi.org/10.1016/j.envint.2017.12.012

Barbeau D, Maitre A, Marques M (2011) Highly sensitive routine method for urinary 3-hydroxybenzo[a]pyrene quantitation using liquid chromatography-fluorescence detection and automated off-line solid phase extraction. Analyst 136(6):1183–1191. https://doi.org/10.1039/C0AN00428F

Bickers DR, Kappas A (1978) Human skin aryl hydrocarbon hydroxylase. Induction by coal tar. J Clin Invest 62(5):1061–1068. https://doi.org/10.1172/JCI109211

Boffetta P, Jourenkova N, Gustavsson P (1997) Cancer risk from occupational and environmental exposure to polycyclic aromatic hydrocarbons. Cancer Causes Control 8(3):444–472. https://doi.org/10.1023/a:1018465507029

Bouchard M, Viau C (1996) Urinary excretion kinetics of Pyrene and Benzo(a)pyrene metabolites following intravenous administration of the parent compounds or the metabolites. Toxicol Appl Pharmacol 139(2):301–309. https://doi.org/10.1006/taap.1996.0169

Brinkmann J, Stolpmann K, Trappe S et al (2013) Metabolically competent human skin models: activation and genotoxicity of benzo[a]pyrene. Toxicol Sci 131(2):351–359. https://doi.org/10.1093/toxsci/kfs316

Bronaugh RL, Maibach HI (2005) Percutaneous absorption: drugs, cosmetics, mechanisms, methods. CRC Press, Boca Raton

Bronaugh RL, Stewart RF (1985) Methods for in vitro percutaneous absorption studies IV: the flow-through diffusion cell. J Pharm Sci 74(1):64–67

Bronaugh RL, Stewart RF (1986) Methods for in vitro percutaneous absorption studies VI: preparation of the Barrier layer. J Pharm Sci 75(5):487–491. https://doi.org/10.1002/jps.2600750513

Cavet M, Leonard M (2013) Les expositions aux produits chimiques cancérogènes en 2010. Dares Anal 54:9

Cheung C, Smith CK, Hoog J-O, Hotchkiss SAM (1999) Expression and localization of human alcohol and aldehyde dehydrogenase enzymes in skin. Biochem Biophys Res Commun 261(1):100–107. https://doi.org/10.1006/bbrc.1999.0943

Chu I, Dick D, Bronaugh R, Tryphonas L (1996) Skin reservoir formation and bioavailability of dermally administered chemicals in hairless guinea pigs. Food Chem Toxicol 34(3):267–276. https://doi.org/10.1016/0278-6915(95)00112-3

Farahmand S, Maibach HI (2009) Transdermal drug pharmacokinetics in man: interindividual variability and partial prediction. Int J Pharma 367(1–2):1–15. https://doi.org/10.1016/j.ijpharm.2008.11.020

Fernando S, Shaw L, Shaw D et al (2016) Evaluation of firefighter exposure to wood smoke during training exercises at burn houses. Environ Sci Technol 50(3):1536–1543. https://doi.org/10.1021/acs.est.5b04752

Flaten GE, Palac Z, Engesland A, Filipović-Grčić J, Vanić Ž, Škalko-Basnet N (2015) In vitro skin models as a tool in optimization of drug formulation. Eur J Pharm Sci 75:10–24. https://doi.org/10.1016/j.ejps.2015.02.018

Fustinoni S, Campo L, Cirla PE et al (2010) Dermal exposure to polycyclic aromatic hydrocarbons in asphalt workers. Occup Environ Med 67(7):456–463. https://doi.org/10.1136/oem.2009.050344

Förster K, Preuss R, Roßbach B, Brüning T, Angerer J, Simon P (2008) 3-Hydroxybenzo[a]pyrene in the urine of workers with occupational exposure to polycyclic aromatic hydrocarbons in different industries. Occup Environ Med 65(4):224–229. https://doi.org/10.1136/oem.2006.030809

Genies C, Maître A, Lefèbvre E, Jullien A, Chopard-Lallier M, Douki T (2013) The extreme variety of genotoxic response to Benzo[a]pyrene in three different human cell lines from three different organs. PloS one 8(11):e78356. https://doi.org/10.1371/journal.pone.0078356

Hecht SS, Carmella SG, Villalta PW, Hochalter JB (2010) Analysis of phenanthrene and Benzo[a]pyrene tetraol enantiomers in human urine: relevance to the bay region diol epoxide hypothesis of Benzo[a]pyrene carcinogenesis and to biomarker studies. Chem Res Toxicol 23(5):900–908. https://doi.org/10.1021/tx9004538

Hewitt NJ, Edwards RJ, Fritsche E et al (2013) Use of human in vitro skin models for accurate and ethical risk assessment: metabolic considerations. Toxicol Sci 133(2):209–217. https://doi.org/10.1093/toxsci/kft080

Hopf NB, Spring P, Hirt-Burri N et al (2018) Polycyclic aromatic hydrocarbons (PAHs) skin permeation rates change with simultaneous exposures to solar ultraviolet radiation (UV-S). Toxicol Lett 287:122–130. https://doi.org/10.1016/j.toxlet.2018.01.024

IARC (2010) Some non-heterocyclic polycyclic aromatic hydrocarbons and some related exposures. IARC monographs on the evaluation of carcinogenic risks to humans/World Health Organization. Int Agency Res Cancer 92:1–853

Ibrahim SA, Li SK (2009) Effects of solvent deposited enhancers on transdermal permeation and their relationship with Emax. J Controlled Release 136(2):117–124. https://doi.org/10.1016/j.jconrel.2009.01.023

Jacques C, Perdu E, Duplan H et al (2010) Disposition and biotransformation of 14C-Benzo(a)pyrene in a pig ear skin model: ex vivo and in vitro approaches. Toxicol Lett 199(1):22–33. https://doi.org/10.1016/j.toxlet.2010.08.001

Jongeneelen FJ (2001) Benchmark guideline for urinary 1-hydroxypyrene as biomarker of occupational exposure to polycyclic aromatic hydrocarbons. Ann Occup Hyg 45(1):3–13. https://doi.org/10.1093/annhyg/45.1.3

Kammer R, Tinnerberg H, Eriksson K (2011) Evaluation of a tape-stripping technique for measuring dermal exposure to pyrene and benzo(a)pyrene. J Environ Monit 13(8):2165–2171. https://doi.org/10.1039/C1EM10245A

Kao J, Patterson FK, Hall J (1985) Skin penetration and metabolism of topically applied chemicals in six mammalian species, including man: an in vitro study with benzo[a]pyrene and testosterone. Toxicol Appl Pharmacol 81(3 Pt 1):502–516

Kontir DM, Glance CA, Colby HD, Miles PR (1986) Effects of organic solvent vehicles on benzo[a]pyrene metabolism in rabbit lung microsomes. Biochem Pharmacol 35(15):2569–2575. https://doi.org/10.1016/0006-2952(86)90055-9

Lehman PA, Raney SG, Franz TJ (2011) Percutaneous absorption in man: in vitro-in vivo correlation. Skin Pharmacol Physiol 24(4):224–230

Liddle C, Goodwin BJ, George J, Tapner M, Farrell GC (1998) Separate and interactive regulation of cytochrome P450 3A4 by triiodothyronine, dexamethasone, and growth hormone in cultured hepatocytes1. J Clin Endocrinol Metabol 83(7):2411–2416. https://doi.org/10.1210/jcem.83.7.4877

Lutier S, Maître A, Bonneterre V et al (2016) Urinary elimination kinetics of 3-hydroxybenzo(a)pyrene and 1-hydroxypyrene of workers in a prebake aluminum electrode production plant: Evaluation of diuresis correction methods for routine biological monitoring. Environ Res 147:469–479. https://doi.org/10.1016/j.envres.2016.02.035

Mcclean M, Rinehart R, Herrick R (2006) Dermal exposure and urinary 1-hydroxypyrene among asphalt roofing workers. Epidemiology 17(6):S134–S135

Moody RP, Nadeau B, Chu I (1995) In vivo and in vitro dermal absorption of benzo[a]pyrene in rat, guinea pig, human and tissue-cultured skin. J Dermatol Sci 9(1):48–58

Moody RP, Yip A, Chu I, Glycol E (2009) Effect of cold storage on in vitro human skin absorption of six 14C-radiolabeled environmental contaminants: Benzo[a]Pyrene. methyl parathion, naphthalene, nonyl phenol, and toluene. J Toxicol Environ Health Part A 72(8):505–517. https://doi.org/10.1080/15287390802328713

Moorthy B, Chu C, Carlin DJ (2015) Polycyclic aromatic hydrocarbons: from metabolism to lung cancer. Toxicol Sci 145(1):5–15. https://doi.org/10.1093/toxsci/kfv040

Moreau M, Bouchard M (2014) Comparison of the kinetics of various biomarkers of benzo[a]pyrene exposure following different routes of entry in rats. J Appl Toxicol 35(7):781–790. https://doi.org/10.1002/jat.3070

Ng KM, Chu I, Bronaugh RL, Franklin CA, Somers DA (1992) Percutaneous absorption and metabolism of pyrene, benzo[a]pyrene, and di(2-ethylhexyl) phthalate: comparison of in vitro and in vivo results in the hairless guinea pig. Toxicol Appl Pharmacol 115(2):216–223

Ngo MA, Maibach HI (2010) Dermatotoxicology: Historical perspective and advances. Toxicol Appl Pharmacol 243(2):225–238. https://doi.org/10.1016/j.taap.2009.12.008

Payan JP, Lafontaine M, Simon P et al (2009) 3-Hydroxybenzo(a)pyrene as a biomarker of dermal exposure to benzo(a)pyrene. Arch Toxicol 83(9):873–883. https://doi.org/10.1007/s00204-009-0440-0

Penning TM (2014) Human Aldo-Keto reductases and the metabolic activation of polycyclic aromatic hydrocarbons. Chem Res Toxicol 27(11):1901–1917. https://doi.org/10.1021/tx500298n

Pinheiro JC, Bates DM (2000) Mixed-effects models in S and S-PLUS. Springer, New York, pp 528

Plakunov I, Smolarek TA, Fischer DL, Wiley JC Jr, Baird WM (1987) Separation by ion-pair high-performance liquid chromatography of the glucuronide, sulfate and glutathione conjugates formed from benzo[a]pyrene in cell cultures from rodents, fish and humans. Carcinogenesis 8(1):59–66

van de Sandt JJM, van Burgsteden JA, Cage S et al (2004) In vitro predictions of skin absorption of caffeine, testosterone, and benzoic acid: a multi-centre comparison study. Regul Toxicol Pharmacol 39(3):271–281. https://doi.org/10.1016/j.yrtph.2004.02.004

Sartorelli P, Aprea C, Cenni A et al (1998) Prediction of percutaneous absorption from physicochemical data: a model based on data of in vitro experiments. Ann Occup Hyg 42(4):267–276

Schwarz D, Kisselev P, Cascorbi I, Schunck WH, Roots I (2001) Differential metabolism of benzo[a]pyrene and benzo[a]pyrene-7,8-dihydrodiol by human CYP1A1 variants. Carcinogenesis 22(3):453–459

Shimada T (2006) Xenobiotic-metabolizing enzymes involved in activation and detoxification of carcinogenic polycyclic aromatic hydrocarbons. Drug Metabol Pharmacokinet 21(4):257–276

Sobus JR, McClean MD, Herrick RF et al (2009) Comparing urinary biomarkers of airborne and dermal exposure to polycyclic aromatic compounds in asphalt-exposed workers. Ann Occup Hyg 53(6):561–571. https://doi.org/10.1093/annhyg/mep042

Storm JE, Collier SW, Stewart RF, Bronaugh RL (1990) Metabolism of xenobiotics during percutaneous penetration: role of absorption rate and cutaneous enzyme activity. Fundam Appl Toxicol 15(1):132–141

VanRooij JG, Bodelier-Bade MM, Jongeneelen FJ (1993a) Estimation of individual dermal and respiratory uptake of polycyclic aromatic hydrocarbons in 12 coke oven workers. Br J Ind Med 50(7):623–632

VanRooij JGM, De Roos JHC, Bodelier-Bade MM, Jongeneelen FJ (1993b) Absorption of polycyclic aromatic hydrocarbons through human skin: differences between anatomical sites and individuals. J Toxicol Environ Health 38(4):355–368. https://doi.org/10.1080/15287399309531724

VanRooij JGM, Bodelier-Bade M, De Looff M, Dijkmans AJA, Jongeneelen APGF (1992) Dermal exposure to polycyclic aromatic hydrocarbons among primary aluminium workers. La Medicina del lavoro 83(5):519–529

Xue W, Warshawsky D (2005) Metabolic activation of polycyclic and heterocyclic aromatic hydrocarbons and DNA damage: a review. Toxicol Appl Pharmacol 206(1):73–93. https://doi.org/10.1016/j.taap.2004.11.006

Zanger UM, Schwab M (2013) Cytochrome P450 enzymes in drug metabolism: Regulation of gene expression, enzyme activities, and impact of genetic variation. Pharmacol Ther 138(1):103–141. https://doi.org/10.1016/j.pharmthera.2012.12.007

Zhong Y, Carmella SG, Hochalter JB, Balbo S, Hecht SS (2011) Analysis of r-7,t-8,9,c-10-Tetrahydroxy-7,8,9,10-tetrahydrobenzo[a]pyrene in Human Urine: a biomarker for directly assessing carcinogenic polycyclic aromatic hydrocarbon exposure plus metabolic activation. Chem Res Toxicol 24(1):73–80. https://doi.org/10.1021/tx100287n